

Characterization of Fluctuations of Impedance and Scattering Matrices in Wave Chaotic Scattering

Xing Zheng, Sameer Hemmady, Thomas M. Antonson Jr., Steven M. Anlage, and Edward Ott
 Department of Physics
 and Institute for Research in Electronics and Applied Physics,
 University of Maryland, College Park, MD, 20742
 (dated: November 10, 2019)

In wave chaotic scattering, statistical fluctuations of the scattering matrix S and the impedance matrix Z depend both on universal properties and on nonuniversal details of how the scatterer is coupled to external channels. This paper considers the impedance and scattering variance ratios, VR_z and VR_s , where $VR_z = \text{Var}[Z_{ij}] / \sqrt{\text{Var}[Z_{ii}] \text{Var}[Z_{jj}]}$, $VR_s = \text{Var}[S_{ij}] / \sqrt{\text{Var}[S_{ii}] \text{Var}[S_{jj}]}$, and $\text{Var}[\cdot]$ denotes variance. VR_z is shown to be a universal function of distributed losses within the scatterer. That is, VR_z is independent of nonuniversal coupling details. This contrasts with VR_s for which universality applies only in the large loss limit. Explicit results are given for VR_z for time reversal symmetric and broken time reversal symmetric systems. Experimental tests of the theory are presented using data taken from scattering measurements on a chaotic microwave cavity.

Keywords: wave transport, chaotic scattering

I. INTRODUCTION

The general problem of externally generated time harmonic waves linearly interacting with a structure of limited spatial extent is basic in many fields of science [1, 2, 3]. In recent years much work has been done elucidating the consequences for the scattering of waves in cases in which, in the geometric optics approximation, the ray orbits within the structure are chaotic. Examples include optical [4], acoustic [5], microwave [6, 7, 8, 9] and electronic cavities [10, 11]. In the case of complex or irregularly shaped enclosures that are large compared with a wavelength, small changes in the frequency and the conformation give rise to large changes in the scattering characteristics. This feature motivates treatments that are statistical in nature. In this regard random matrix theory [12, 13] has proven useful in predicting universal aspects of chaotic wave scattering problems in the cases of both time reversal symmetric systems (corresponding to matrix statistics of the Gaussian Orthogonal Ensemble, GOE) and time reversal symmetry broken systems (corresponding to matrix statistics of the Gaussian Unitary Ensemble, GUE).

Scattering problems can be characterized by the scattering matrix S which relates outgoing scattered wave amplitudes b to incoming waves a , via $b = Sa$. An alternative formulation is in terms of the impedance matrix Z . To illustrate the impedance description, consider an electromagnetic wave scattering problem in which N transmission lines labeled $i = 1, 2, \dots, N$ of characteristic impedance Z_{0i} are connected to a cavity. Let V_i and I_i represent the voltage and current on transmission line i as measured at a suitable reference plane. Then the incident wave a_i and the reflected wave b_i may be expressed

as $a_i = (V_i + Z_{0i}I_i)/Z_{0i}$, $b_i = (V_i - Z_{0i}I_i)/Z_{0i}$. The impedance matrix Z relates the vector voltage to the vector current, via $V = ZI$, and Z and S are related by $Z = Z_0^{1/2} (1 - S)^{-1} (1 + S) Z_0^{1/2}$, where 1 is the N -dimensional identity matrix, and $Z_0 = \text{diag}(Z_{01}, Z_{02}, \dots, Z_{0N})$. The impedance formulation is identical to the so-called "R-matrix", a formulation introduced by Wigner and Eisenbud in nuclear-reaction theory in 1947, and further developed in Refs. [14, 15, 16, 17].

Statistical variations of the elements of Z and S due to small random variations in the scatterer are of great interest. These statistics have two fundamental features, (i) universal aspects described by random matrix theory, and (ii) nonuniversal aspects dependent upon the details of the coupling of input channels (e.g., transmission lines) to the scatterer. Our main result concerns the quantity,

$$VR_z = \frac{\text{Var}[Z_{ij}]}{\sqrt{\text{Var}[Z_{ii}] \text{Var}[Z_{jj}]}}; \quad i \neq j; \quad (1)$$

where $\text{Var}[A]$, the variance of the complex scalar A , is defined as the sum of $\text{Var}[\text{Re}A]$ and $\text{Var}[\text{Im}A]$. Our result is of the form

$$VR_z = \begin{cases} F_1(\gamma) & \text{for GOE,} \\ F_2(\gamma) & \text{for GUE,} \end{cases} \quad (2)$$

where γ is a parameter characterizing the losses within the scatterer. For example, in the case of an electromagnetic cavity, $\gamma = \pi/(2Q\lambda)$, where λ is the frequency of the incoming signal, λ is the average spacing between cavity resonant frequencies near λ , and Q is the quality factor of the cavity ($Q = 1$ if there are no internal losses). The remarkable aspect of (2) is that $F_{1,2}(\gamma)$ depends only on the loss parameter and not on the nonuniversal properties of the coupling to the cavity. Thus VR_z is a universal function of the loss γ . The results for F_1 and F_2 (to be derived subsequently) are shown in Fig. 1.

Also at Department of Electrical and Computer Engineering.

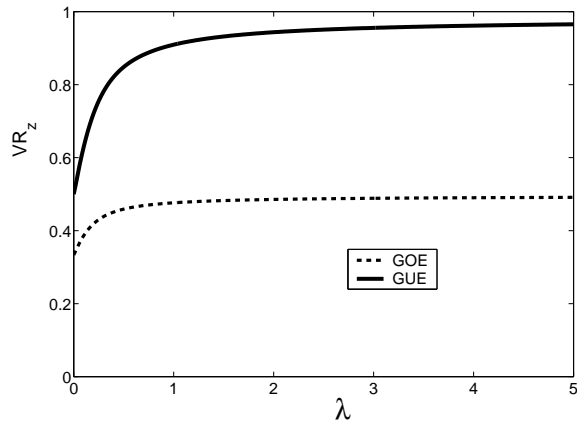


FIG. 1: VR_z versus the loss parameter λ , as specified in Eq. (15) and Eq. (16).

For $\lambda \ll 1$,

$$VR_z = \begin{cases} 1=2 & \text{for GOE,} \\ 1 & \text{for GUE.} \end{cases} \quad (3)$$

For $\lambda \gg 1$,

$$VR_z = \begin{cases} 1=3 & \text{for GOE,} \\ 1=2 & \text{for GUE.} \end{cases} \quad (4)$$

A ratio similar to (1) can also be considered for the scattering matrix S ,

$$VR_s = \frac{\text{Var}[S_{ij}]}{\text{Var}[S_{ii}]\text{Var}[S_{jj}]}; \quad i \neq j: \quad (5)$$

In contrast with (2), VR_s in general depends on both the coupling to the cavity and on the loss parameter λ . However, in the special case of high loss, $\lambda \gg 1$, VR_s becomes universal,

$$VR_s = \begin{cases} 1=2 & \text{for GOE,} \\ 1 & \text{for GUE.} \end{cases} \quad (6)$$

That is, $VR_s = VR_z$ for $\lambda \gg 1$. Based on their electromagnetic experiments, Fiacchetti and Michelsen [18] have recently conjectured the universality of (6) in the GOE case. More generally, (6) follows from classic results of Hauser and Feshbach describing fluctuations in the cross section of inelastic neutron scattering [19], and this result has been obtained by Friedman and Melb [20] using the concept of maximization of information entropy, and by Agassi et al. [21] using a random matrix model. The important point is that a universal result for VR_s [i.e., Eq. (6)] applies only for $\lambda \gg 1$, while the universal result for VR_z , Eq. (2) and Fig. 1, is for arbitrary λ .

In what follows we derive these results and test them by comparison with data obtained from scattering measurements on a chaotic microwave cavity. Section II derives the results for impedance variance ratio, VR_z . Section III considers the scattering variance ratio, VR_s . Section IV presents our experimental tests of the theory.

II. IMPEDANCE VARIANCE RATIO

In this section we will obtain the universal functions $F_{1,2}(\lambda)$ in Eq. (2). We adopt a formulation (e.g., see Refs. [22, 24]) that incorporates the nonuniversal effects of the specific coupling geometry of input-output channels to the scatterer, combined with the random matrix theory for the universal aspects of the chaotic wave behavior within the scatterer. (In what follows, we use terminology appropriate to microwave experiments.) Beginning with the case of zero loss ($\lambda = 0$), we have that, in the GOE case, the impedance matrix Z is described by the following statistical model [24],

$$Z = \frac{j}{k} \sum_n^X \frac{R_r^{1=2}(k_n) w_n w_n^T R_r^{1=2}(k_n)}{k^2 - k_n^2}: \quad (7)$$

Here k is the wave number corresponding to the incoming frequency, w_n is a vector whose elements are real, independent, zero mean, Gaussian random variables of unit variance. The eigenvalues k_n^2 are randomly chosen with statistics appropriate to GOE. This is done by generating ensembles of eigenvalues of random matrices and then scaling them such that the mean spacing between adjacent eigenvalues near k_n^2 is λ_n . For the case of a 2D cavity $\lambda_n = 4/A$ where A is the area of the cavity. The system-dependent part of the coupling is characterized by the corresponding radiation impedance matrix $Z_r = R_r + jX_r$. Note also that, since Z_r depends only on local geometry near the entrances to the scattering region, its frequency dependence is much slower than that of Z which depends on the geometry of the scattering region assumed to be characterized by much longer length scales. The radiation impedance is the impedance seen at the reference plane of the input channel when waves that leave the channel propagate outward and are not reflected back to their input by the distant walls of the cavity. Thus the radiation impedance is the impedance seen when the distant walls are removed to infinity, or (as can be done in an experimental measurement [9]) when the distant walls are lined with absorber. Hence the radiation impedance depends only on the local structure in the vicinity of the port coupling to the cavity and not on the shape or chaotic properties of the cavity. In the case of ports that are far apart, e.g., of the order of the cavity size, the off-diagonal elements of Z_r are small and will be neglected. Thus we will take Z_r to be a diagonal matrix with elements $Z_{ri} = R_{ri} + jX_{ri}$. In the GUE case, the elements of w_n in (7) are complex with real and imaginary parts each individually having Gaussian statistics, w_n^T in (7) is replaced by w_n^Y (where Y denotes the conjugate transpose), and the statistics of k_n^2 are now those appropriate to GUE. We note that in Eq. (7) the statistical properties of the quantities $k_n^2 = \lambda_n$ and w_n are assumed to be universal while Z_r (and hence R_r) depends on the nonuniversal geometry-dependent details of the coupling structures at the input to the scatterer.

The universality of the result for VR_z (Fig. 1) can

be simply seen from (7) as follows. First we note that $Z_r(k)$ and hence $R_r(k)$ are slowly varying function of k . Considering a range of k small enough that $Z_r(k)$ may be considered constant, yet large enough that (7) contains many resonances, we have that

$$R_r^{-1/2} Z R_r^{-1/2} = \frac{j}{n} \sum_{n=1}^X \frac{w_n w_n^T}{k^2 k_n^2} : \quad (7')$$

Normalizing k^2, k_n^2 to the mean spacing between eigenvalues (n can be regarded as constant in the above referenced range of k), we see that the right hand side of Eq. (7') contains only universal quantities. Thus $Z' = R_r^{-1/2} Z R_r^{-1/2}$ is universal. If Z_r is diagonal, we have $Z'_{ij} = R_{ri}^{-1/2} R_{rj}^{-1/2} Z_{ij}$. Hence the ratios VR_z defined by (1) is the same for Z and Z' and hence is universal. (We emphasize, however, that this conclusion relies on Z_r being diagonal.)

The effects of distributed loss, such as losses due to conducting walls or a lossy dielectric that fills the cavity, can be simply incorporated in Eq. (7). Since modal fluctuations in losses are small when the modes are chaotic and the wavelength is short, we can construct a complex cavity impedance accounting for distributed loss by simply replacing k^2 in Eq. (7) by $k^2(1 - j/Q)$, where Q is the cavity quality factor. For example,

$$\begin{aligned} Z_{ii} &= \frac{j}{n=1} \sum^X \frac{R_{ri} R_{rn} w_{in}^2}{k^2 (1 - j/Q) k_n^2} R_{ii} + j X_{ii} \\ &= \frac{1}{n=1} \sum^X \frac{R_{ri} R_{rn} w_{in}^2 k^2 = Q}{(k^2 - k_n^2)^2 + (k^2 = Q)^2} + j \sum_{n=1}^X \frac{R_{ri} R_{rn} w_{in}^2 (k_n^2 - k^2)}{(k^2 - k_n^2)^2 + (k^2 = Q)^2} \end{aligned} \quad (8)$$

Calculation of the moments of the impedance is facilitated by the fact that the eigenvalues and eigenfunctions in the chaotic cavities are statistically independent. For example, the expected value of X_{ii} is,

$$\begin{aligned} E[X_{ii}] &= \lim_{M \rightarrow \infty} \frac{1}{M} \sum_{n=1}^M \int dw_{in} f(w_{in}) w_{in}^2 \int dk_1^2 \dots \int dk_M^2 \\ &= P_J(k_1^2; \dots, k_M^2) \int \frac{R_{ri} R_{rn} (k_n^2 - k^2)}{(k^2 - k_n^2)^2 + (k^2 = Q)^2} dk \end{aligned} \quad (9)$$

where $f(w_{in})$ is the probability distribution function (pdf) of w_{in} and P_J is the joint pdf of the eigenvalues. Integrating over all $k_j, j \notin n$, we express $E[X_{ii}]$ as an integral over the pdf of $k_n^2, P_1(k_n^2) = 1/(M)$, we consider the $M \rightarrow \infty$ limit and use $hw_n^2 = 1$ for the Gaussian random variable w_n .

$$E[X_{ii}] = \int dk_n^2 \frac{R_{ri} R_{rn} (k_n^2 - k^2)}{(k^2 - k_n^2)^2 + (k^2 = Q)^2} = X_{ri}(k) : \quad (10)$$

The second equality in (10) relating $E[X_{ii}]$ to the radiation reactance requires $Q \gg 1$ and is analogous to the Rams-Kronig relation.

The second moment of X_{ii} can be determined in a similar way by integrating over all j except $j = i$; and

using the joint distribution function $P_2(k_c^2; k_s^2) = [g(k_c^2 - k_s^2)]^2 / (M)^2$, where $g(k_c^2 - k_s^2)$ is known from Random Matrix theory [13]. Using the fact that g goes to zero at large argument and assuming that the radiation resistance $R_{ri}(k_n)$ and the average spacing n vary slowly over the damping width $k^2 = Q$, we obtain

$$\begin{aligned} E[X_{ii}^2] &= \frac{3}{2} (R_{ri}^2 \frac{1}{k^2 = Q}) + f E[X_{ii}]^2 + \frac{R_{ri}^2}{2} \int dk_c^2 dk_s^2 \\ &= \frac{hw^2 i^2 g(k_c^2 - k_s^2) (k_c^2 - k^2) (k_s^2 - k^2)}{[(k_c^2 - k^2)^2 + (k^2 = Q)^2][(k_s^2 - k^2)^2 + (k^2 = Q)^2]} \end{aligned} \quad (11)$$

Combining Eq. (11) and Eq. (10), we obtain

$$\text{Var}[X_{ii}] = \frac{R_{ri}^2}{2} \left[\frac{3}{2} - \frac{1}{0} \int dx g(x) \frac{4}{4 + (x =)^2} \right] \quad (12)$$

where $x = k^2 - Q$. A similar moment evaluation can be carried out for R_{ii} , as specified in Eq. (8), which yields the same expression as Eq. (12) for $\text{Var}[R_{ii}]$. For GOE (the case we are now considering) we have that [13], $g(s) = f^2(s) \int_0^s d(s^0) f(s^0) = 2 \int (df = ds)$, where $f(s) = [(\sin s) = (s)]$.

In order to obtain the variance ratio, we also apply the previous process to the off-diagonal term $Z_{ij}, i \neq j$, which, based on Eq. (7), is given by

$$\begin{aligned} Z_{ij} &= \frac{1}{n} \sum^X \frac{R_{ri} R_{rj} w_{in} w_{jn} k^2 = Q}{(k^2 = Q)^2 + (k^2 - k_n^2)^2} \\ &+ j \sum_n^X \frac{R_{ri} R_{rj} w_{in} w_{jn} k^2 = Q}{(k^2 = Q)^2 + (k^2 - k_n^2)^2} \end{aligned} \quad (13)$$

Since w_{in} and w_{jn} are independent, the first moments of X_{ij} and R_{ij} are both zero, and the variance is equal to the second moment,

$$\begin{aligned} \text{Var}[X_{ij}] &= \lim_{M \rightarrow \infty} \frac{M}{2} \int dk_n^2 \frac{R_{ri} R_{rj} w_{in}^2 w_{jn}^2}{[(k_n^2 - k^2)^2 + (k^2 = Q)^2]} P_1(k_n^2) \\ &= \frac{R_{ri} R_{rj}}{2} \frac{1}{2} \end{aligned} \quad (14)$$

The same result is obtained for $\text{Var}[R_{ij}]$. Combining Eq. (14) with Eq. (12), we have Eq. (2) with

$$\text{VR}_z = F_1(\lambda) = \left[\frac{3}{2} - \int_0^{\lambda} dx g(x) \frac{4}{4 + (x =)^2} \right]^2 \quad (15)$$

A similar calculation in the GUE case is facilitated by the simpler form of the function $g(x)$ which is now given by $g(x) = \sin^2(x) = (x)^2$. We obtain

$$\begin{aligned} \text{VR}_z &= F_2(\lambda) = \left[\frac{3}{2} - \int_0^{\lambda} dx \left(\frac{\sin x}{x} \right)^2 \frac{4}{4 + (x =)^2} \right]^2 \\ &= \left[1 + \frac{1}{4} e^{-4} \right]^2 \end{aligned} \quad (16)$$

We note that the two-frequency correlation functions for the elements of the impedance and the scattering matrix have recently been calculated by Savin, Fyodorov and Sommers [25], and are consistent with the preceding in the limit of zero frequency separation.

III. SCATTERING VARIANCE RATIO

We now consider the scattering matrix in the high loss limit, $\gamma_r = 1$. For simplicity, we consider the case of two channels connecting to the scatterer, $N = 2$, and Z and S are 2×2 matrices. We note that a chaotic scattering process can be divided into a direct process and a delayed process, which leads to a separation of the mean part (equal to Z_r) and the fluctuating part Z of the cavity impedance, $Z = Z_r + Z$. The fluctuating part Z decreases as loss increases. Thus in the high loss limit, $Z \rightarrow Z_r$, which implies $Z_{12}; Z_{21} \rightarrow Z_{11}; Z_{22}$. (Recall, the mean parts of the off-diagonal components are zero.) We may now form S using $S = Z_0^{-1/2} (Z + Z_0)^{-1} Z_0^{1/2}$. Since the off-diagonal terms of Z are small, the diagonal components of S are dominated by the diagonal components of Z . We then find for S_{11} ,

$$\begin{aligned} S_{11} &= \frac{Z_{11} - Z_{01}}{Z_{11} + Z_{01}} = \frac{(Z_{r1} - Z_{01}) + Z_{11}}{(Z_{r1} + Z_{01}) + Z_{11}} \\ &= S_{r1} + \left[\frac{2Z_{01}}{(Z_{r1} + Z_{01})^2} \right] Z_{11}; \end{aligned} \quad (17)$$

where $S_{r1} = (Z_{r1} - Z_{01}) / (Z_{r1} + Z_{01})$, and Z_{01} is the characteristic impedance of channel 1. Thus, we obtain

$$\text{Var}[S_{11}] = \frac{2Z_{01}}{(Z_{r1} + Z_{01})^2} \int \text{Var}[Z_{11}]; \quad (18)$$

In addition, we can express S_{12} in the high damping limit as

$$S_{12} = \frac{2Z_{12} \frac{p}{Z_{01}Z_{02}}}{(Z_{11} + Z_{01})(Z_{22} + Z_{02})}, \quad \frac{2Z_{12} \frac{p}{Z_{01}Z_{02}}}{(Z_{r1} + Z_{01})(Z_{r2} + Z_{02})}; \quad (19)$$

which leads to

$$\text{Var}[S_{12}] = \frac{2 \frac{p}{Z_{01}Z_{02}}}{(Z_{r1} + Z_{01})(Z_{r2} + Z_{02})} \int \text{Var}[Z_{12}]; \quad (20)$$

and similarly for $\text{Var}[S_{21}]$. Combining Eq. (18) and Eq. (20), we recover Eq. (6) and we note that this result is independent of the coupling (i.e., independent of Z_r).

To illustrate the influence of coupling on VR_s at finite loss parameter γ , we consider the impedance matrix in the GOE case using the model normalized impedance used in Ref. [22], $Z = \frac{1}{p} R_r^{1/2} R_r^{1/2} + jX_r$, where X_r is given by $X_{ij} = \frac{1}{p} \sum_{n=1}^M (w_{in} w_{jn}) = (\mathcal{K}^2 \mathcal{K}_n^2 - j)$, $\mathcal{K}_n^2 = k^2 = \gamma$, and \mathcal{K}^2 is set to be $M/2$, such that mean of X is zero. Realizations of X are produced numerically by

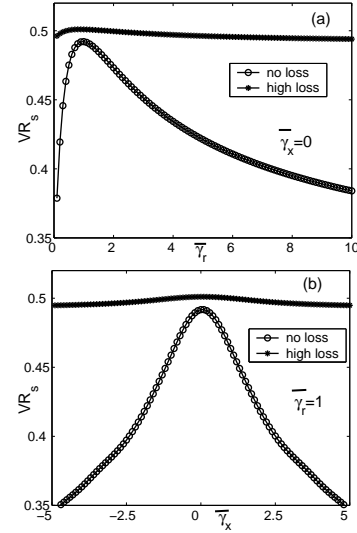


FIG. 2: (a) VR_s versus γ_r for $\gamma_x = 0$ in the lossless case ($\gamma = 0$) and in a high loss case ($\gamma = 5$). (b) VR_s versus γ_x for $\gamma_r = 1$.

generating Gaussian random variables w_{in} and spectra \mathcal{K}_n^2 from the eigenvalues of random matrices. We express a model scattering matrix S as

$$S = \left(\frac{1}{r} \frac{1}{r} + j \gamma_x + 1 \right)^{-1} \left(\frac{1}{r} \frac{1}{r} + j \gamma_x - 1 \right); \quad (21)$$

where $r = Z_0^{-1} R_r$ and $x = Z_0^{-1} X_r$. When r is the identity matrix and x is zero, we reach the so-called perfect coupling condition, which means that the scattering is determined by the delayed process and the direct process is absent. We now consider an example in which the two-port couplings are the same so that $r_{jk} = \text{diag}(r_{jk}; r_{jk})$, where r_{jk} is a scalar. Figures 2(a) and (b) show results for the variation of VR_s with the coupling parameters γ_r and γ_x , for a high loss case ($\gamma = 5$) and for the lossless case ($\gamma = 0$). In Fig. 2(a), we γ_x to be zero, and vary γ_r , while in Fig. 2(b), γ_r is fixed to be 1 and γ_x is varied. Compared to the high damping case, VR_s in the lossless case has a much larger deviation from the constant 1/2. Note that VR_s is 1/2 in the perfect-coupling case (i.e., $r = 1$, $x = 0$), no matter whether the cavity is highly lossy or lossless. This is related to the concept of "weak localization" reviewed in [23].

In the case of an N -port we can think of the above two-port consideration of VR_s as applying to the N -port converted to a two port by opening channels 3;4; ...;N; i.e., the incoming waves $a_3; a_4; \dots; a_N$ are identically zero (for a microwave cavity with transmission line inputs, this corresponds to terminating transmission lines 3;4; ...;N with their characteristic impedances, $Z_{03}; Z_{04}; \dots; Z_{0N}$). Thus ports 3;4; ...;N effectively add to the loss due to the energy flux leaving through them. If the ports 3;4; ...;N are assumed to act like distributed loss, they can be taken into account by increasing the loss parameter γ . [This increased loss enhances the validity of Eq. (6).]

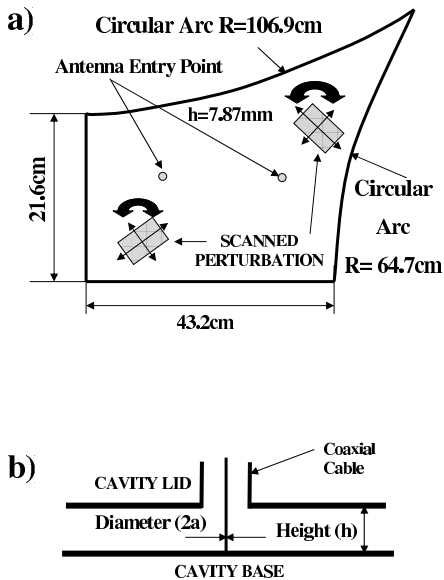


FIG. 3: (a) The physical dimensions of quarter bow-tie chaotic microwave resonator are shown along with the position of the two coupling ports. Two metallic perturbations are shown in gray. (b) The details of the coupling ports (antennas) and cavity height h are shown in cross section.

IV. EXPERIMENTAL TESTS

We provide experimental results testing the theoretical predictions for the statistical fluctuations in the variance of the S and Z elements, in the limit of large damping. The experiments are done in an air-filled, quarter bow-tie shaped cavity which acts as a two-dimensional resonator below 19 GHz (Fig. 3 (a)) [26]. This cavity has previously been used for the successful study of the eigenvalue spacing statistics [27], eigenfunction statistics [28, 29], and for studying the universal fluctuations in the impedance [9] and scattering matrix [30] for a wave chaotic system. The cavity is driven by two ports; each of which consists of the center conductor (diameter $2a = 1.27\text{m}$) of a coaxial cable that extends from the top lid of the cavity and makes contact with the bottom plate of the cavity (Fig. 3 (b)). We estimate that our cavity has a typical loaded Q of about 200 in the entire frequency range 7.2 GHz to 8.4 GHz from a direct S_{21} measurement. This translates to a damping parameter of $\gamma \approx 1$ for the frequency range of this experiment. Hence we examine experimentally the time-reversal symmetric (GOE) cases for the Z and S -variance ratios in the high damping limit.

To perform ensemble averaging, two perturbations (shown in gray in Fig. 3 (a)), made up of rectangular ferromagnetic solids wrapped in Al foil (of dimensions $26.7 \times 40.6 \times 7.87\text{mm}^3$), are systematically scanned and rotated throughout the volume of the cavity by means of a magnet that is placed outside the cavity. The ensemble set consists of one-hundred different positions and orientations of the perturbations within the cavity. The perturbations are on the

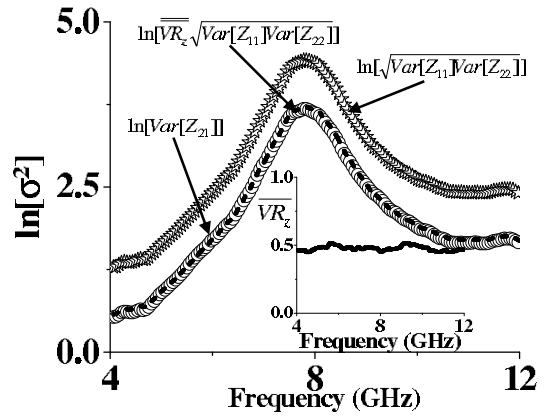


FIG. 4: $\overline{\text{Var}[Z_{21}]}$ (circles), $\overline{\text{Var}[Z_{11}]\text{Var}[Z_{22}]}$ (stars) and $\overline{\text{Var}[Z_{11}]\text{Var}[Z_{22}]}$ (dots) are plotted on a Log scale as a function of frequency from 4 to 12 GHz. Inset shows the ratio $\overline{VR_z}$ versus frequency.

scale of half the wavelength or bigger over the entire frequency range of the experiment, and their 100 different positions and orientations lead to effective ensemble averaging. The full two-by-two S matrix is measured between 4 and 12 GHz for each position of the perturbations. Below 4 GHz the mode density is too low to obtain meaningful ensemble averaging, while above 12 GHz the coupling becomes too weak to couple to the modes of the cavity, at least for this port geometry. Once the S matrix has been measured, it is then converted to Z through $Z = Z_0(I + S)(I - S)^{-1}$.

In order to further improve the statistics, we make use of frequency averaging over a sliding window of width 300 MHz. We denote such sliding averages of impedance and scattering variance ratios by $\overline{VR_z}$ and $\overline{VR_s}$. The inset in Fig. 4 shows $\overline{VR_z}$ over a frequency range 4 GHz to 12 GHz. Denoting the average of $\overline{VR_z}$ over the entire range (4 GHz-12 GHz), by $\overline{\overline{VR_z}}$, we obtain $\overline{\overline{VR_z}} = 0.49$, and we find that $\overline{\overline{VR_z}} - \overline{\overline{VR_z}} < 0.02$ over the entire frequency range. This value of experimentally obtained $\overline{\overline{VR_z}}$ is close to the ideal theoretical value of 1/2 for large damping. The circles, stars and dots in Fig. 4 show the variation in $\ln[\overline{\text{Var}[Z_{21}]}]$ and $\ln[\overline{\text{Var}[Z_{11}]\text{Var}[Z_{22}]}]$ and $\ln[\overline{\overline{\text{Var}[Z_{11}]\text{Var}[Z_{22}]}}]$ respectively, as a function of frequency. Here $\overline{VR_z}$ is taken to be the experimentally average value of 0.49. The agreement is quite good (i.e., the dots overlap the open circles) at all frequencies where effective ensemble averaging can be performed.

Similarly in Fig. 5, we present data for the scattering variance ratio. Experimentally we obtain $\overline{\overline{VR_s}} = 0.50$ and $\overline{\overline{VR_s}} - \overline{\overline{VR_s}} < 0.02$ over the range 4 GHz to 12 GHz. The circles, stars and dots in Fig. 5 show the variation in $\overline{\text{Var}[S_{21}]}$, $\overline{\text{Var}[S_{11}]\text{Var}[S_{22}]}$ and $\overline{\overline{\text{Var}[S_{11}]\text{Var}[S_{22}]}}$, respectively, as a function of frequency. Here $\overline{VR_s}$ is taken to be the experimentally average value of 0.5. Similar to the

